@BoneJointRes

Identification of the molecular link: *STAT3* is a shared key gene linking postmenopausal osteoporosis and sarcopenia

From First Hospital of China Medical University, Shenyang, China

D. Liu,[1] K. Wang,[1] J. Wang,[1] F. Cao,[1] L. Tao[1]

Department of Orthopedics, First Hospital of China Medical University, Shenyang, China

Cite this article:
Bone Joint Res 2024;13(8):
411–426.

DOI: 10.1302/2046-3758.
138.BJR-2023-0351.R2

Correspondence should be sent to Lin Tao taolindr@163.com

Aims

This study explored the shared genetic traits and molecular interactions between postmenopausal osteoporosis (POMP) and sarcopenia, both of which substantially degrade elderly health and quality of life. We hypothesized that these motor system diseases overlap in pathophysiology and regulatory mechanisms.

Methods

We analyzed microarray data from the Gene Expression Omnibus (GEO) database using weighted gene co-expression network analysis (WGCNA), machine learning, and Kyoto Encyclopedia of Genes and Genomes (KEGG) enrichment analysis to identify common genetic factors between POMP and sarcopenia. Further validation was done via differential gene expression in a new cohort. Single-cell analysis identified high expression cell subsets, with mononuclear macrophages in osteoporosis and muscle stem cells in sarcopenia, among others. A competitive endogenous RNA network suggested regulatory elements for these genes.

Results

Signal transducer and activator of transcription 3 (*STAT3*) was notably expressed in both conditions. Single-cell analysis pinpointed specific cells with high *STAT3* expression, and microRNA (miRNA)-125a-5p emerged as a potential regulator. Experiments confirmed the crucial role of *STAT3* in osteoclast differentiation and muscle proliferation.

Conclusion

STAT3 has emerged as a key gene in both POMP and sarcopenia. This insight positions *STAT3* as a potential common therapeutic target, possibly improving management strategies for these age-related diseases.

Article focus

- Identify common genetic characteristics between postmenopausal osteoporosis and sarcopenia using bioinformatics approaches.
- Validate whether signal transducer and activator of transcription 3 (*STAT3*) is a shared key gene implicated in both diseases with differential expression analysis and cell experiments.
- Explore the regulatory mechanisms of *STAT3* by constructing a competing endogenous RNA (ceRNA) network.

Key messages

- *STAT3* was identified as a highly expressed gene common to both osteoporosis and sarcopenia through weighted gene coexpression network analysis.
- *STAT3* plays pivotal roles in osteoclast differentiation and muscle cell proliferation, as confirmed by knockdown and overexpression cell studies.
- MicroRNA (miRNA)-125a-5p was predicted as a regulatory factor of *STAT3* and could be a therapeutic target. Single-cell analysis revealed specific cell subsets with high *STAT3* expression in each disease, providing a basis for experimental validation.

Strengths and limitations

- Multiple bioinformatics approaches systematically analyzed datasets from

Bone & Joint Research

Gene Expression Omnibus (GEO) to identify *STAT3*.
- Findings were validated with differential expression analysis in a separate cohort and experimental cell studies. ceRNA network provided insights into potential regulatory mechanisms of *STAT3*.
- This study was limited to computational analysis of existing datasets, so further mechanistic studies are needed. Specific signalling pathways involving *STAT3* require further elucidation.

Introduction

Postmenopausal osteoporosis (POMP) is the most common motor system disease in postmenopausal women and is characterized by decreased bone mass and bone microstructure disorders, which exist in more than 50% of postmenopausal women.[1] Sarcopenia is a kind of motor system disease related to ageing that mainly manifests as a decrease in muscle mass and muscle strength. Sarcopenia increases the risk of falls and fractures in the elderly, and affects quality of life and self-care ability.[2] To date, dual-energy X-ray absorptiometry has been used to assess POMP and sarcopenia.[3] Overall, 68% of women diagnosed with sarcopenia suffer from osteoporosis.[4] Coin et al[5] reported a positive correlation between bone mineral density (BMD) and muscle mass; that is, patients with low BMD also have less muscle mass. The term "osteosarcopenia" has been used in patients with both sarcopenia and osteoporosis. Therefore, these two diseases often do not exist independently, and there is a close relationship between them.

An increasing number of studies have found that bone and muscle, as two important parts of the motor system, are regulated by a variety of common factors.[6] Muscle cells and bone cells both come from mesenchymal progenitor cells, at the earliest stage of cell development.[7] After maturity, the two are not only neighbours, but also have endocrine regulatory hormones, molecular signalling pathways, and common therapeutic drugs, which affect their respective metabolisms.[8] There is a close relationship between muscle and bone. On the one hand, the mechanical force caused by muscle contraction affects bone growth, bone geometry, and BMD; on the other hand, muscle and bone can regulate each other's synthesis and catabolism by secreting muscle factors and bone factors.[9] As age increases and activity decreases, the levels of these hormones and cytokines decrease, resulting in the weakening of bone and muscle anabolism and an increase in catabolism, muscle hypertrophy/atrophy, and BMD; these losses occur in parallel, leading to osteoporosis and sarcopenia.[10]

However, the existing treatments for POMP or sarcopenia are often aimed at only one disease. The therapeutic effect of osteoporosis therapy is often most obvious within one year of treatment, and 10% to 15% of patients who receive treatment do not experience an increase in bone mass.[11] For sarcopenia, the best treatment is exercise, but its therapeutic effect is not substantial and there is a lack of effective drug treamtents and treatment targets.[12] This phenomenon may be because the pathogeneses of these two diseases are linked, so the treatment of one of the diseases alone cannot achieve good results. The two diseases influence each other, and it may be better to treat them simultaneously. At present, some research progress has been made on these molecular pathways. Muscle secretion of irisin may also be a new common therapeutic target for osteoporosis and sarcopenia.[13] Vitamin D, as a drug to prevent osteoporotic fracture, can effectively treat sarcopenia.[14] Therefore, the two diseases may have common targets, and drugs designed for these targets may alleviate the symptoms of both diseases simultaneously.

In this study, we analyzed microarray data from the Gene Expression Omnibus (GEO) database using weighted gene co-expression network analysis (WGCNA) to identify co-expressed gene modules related to POMP and sarcopenia. We then employed the machine-learning approach random forest to screen for key genes. Differential gene expression analysis was performed to validate the findings in independent datasets. Single-cell RNA sequencing (scRNA-seq) analysis was used to pinpoint the cell type-specific expression patterns of the key gene. Finally, we constructed a competing endogenous RNA (ceRNA) network to explore the potential regulatory mechanism.

Methods

An overall research and design flowchart is shown in Supplementary Figure a.

Data sources and processing

We selected and downloaded datasets related to sarcopenia and osteoporosis from the GEO database (Supplementary Table i). For bulk RNA-seq analysis, we used datasets GSE1428, GSE136344, GSE7158, and GSE56814. These datasets were derived from human skeletal muscle and blood monocytes, with both female and mixed sex samples. For scRNA-seq analysis, we used datasets GSE172410 and GSE147287, which were derived from mouse skeletal muscle and human mesenchymal stem cells, respectively. The sample sizes for control and disease groups are listed in Supplementary Table i.

Data processing was executed using R (version 4.1.3; R Foundation for Statistical Computing, Austria), utilizing packages such as affy,[15] lumi,[16] and sva[17] for normalization, quality assessment, and batch effect removal. Annotation of the gene expression matrix was further refined using the clusterProfiler package.[18]

Gene network and pathway analysis

We applied WGCNA[19] to datasets GSE1428 and GSE56814 for analyzing gene co-expression patterns related to osteoporosis and sarcopenia. Top genes were selected based on standard deviation, followed by sample clustering and module partitioning. Modules were then subjected to Kyoto Encyclopedia of Genes and Genomes (KEGG) enrichment analysis to elucidate their disease associations.[20] Concurrently, we constructed a protein-protein interaction (PPI) network of key genes using the STRING database[21] and identified hub genes via the cytoHubba plugin.[22]

The overlapping genes from the positive correlation modules of GSE1428 and GSE56814 were defined as gene set 1 (GS1), which was considered to be closely related to the pathogenesis of sarcopenia and POMP.

Machine learning and differential expression analysis

GSE136344 and GSE7158 were used as validation datasets to confirm the results obtained from the primary analysis

of GSE1428 and GSE56814. The overlapping differentially expressed genes between GSE136344 and GSE7158 were defined as gene set 2 (GS2), which was used for validation purposes. Random forest analysis was employed to discern disease-related genes.[23] Differential gene expression analysis was conducted using the limma package,[24] and the diagnostic potential of these genes was assessed through receiver operating characteristic (ROC) curves generated with the pROC package.[25]

Single-cell analysis and ceRNA network construction

Single-cell analysis was performed using Seurat,[26] Harmony,[27] and other packages to pinpoint specific cell clusters expressing target genes. ceRNA network construction involved predicting microRNA (miRNA) and long noncoding RNA (lncRNA) targets related to signal transducer and activator of transcription 3 (*STAT3*) using miRanda, miRDB, and TargetScan,[28] with the network visualized in Cytoscape software.[29,30]

Cell culture

RAW264.7 (ATCC, CL-0190) cells and C2C12 (ATCC, CRL-1774) cells were purchased from Procell (China). RAW264.7 cells were cultured in Minimum Essential Medium Alpha (C3064-0500; VivaCell, China), 10% fetal bovine serum (FBS) (BI.04-001-1ACS; Biological Industries, Israel), 1% penicillin/streptomycin, and 5% carbon dioxide at 37°C. C2C12 cells were cultured in Dulbecco's Modified Eagle Medium (DMEM) (C11995500BT; Gibco, Thermo Fisher Scientific, USA), 10% FBS (BI.04-001-1ACS; Biological Industries), 1% penicillin/streptomycin, and 5% carbon dioxide at 37°C.

Cell transfection

STAT3-specific small interfering RNA (siRNA) and overexpression plasmids were obtained from General Biol (China). Lipofectamine 2000 (Invitrogen, Thermo Fisher Scientific) and Opti-MEM (Gibco, 31958-062) were used for siRNA transfection. When the osteoclast progenitor cells or myoblasts reached 40% confluence, siRNA was transfected at a concentration of 50 nM in the presence of transfection reagents. Lipofectamine 2000 and Opti-MEM were used for plasmid transfection. When the osteoclast progenitor cells or myoblasts reached 70% confluence, 10 μg of plasmid was used for transfection in the presence of transfection reagent. The protein was extracted 48 hours after transfection.

Reverse transcription-quantitative polymerase chain reaction

The total RNA of osteoclast progenitor cells or myoblasts was extracted by an RNA Extraction Kit (9767; Takara Bio, Japan), and the extracted RNA was reverse transcribed into complementary DNA (cDNA) by a Prime Script RT kit (RR047A; Takara Bio). Finally, qPCR was performed using TB Green (RR820A; Takara Bio) and a LightCycler480 system (Roche Diagnostics, Switzerland). The sequences of primers used are listed in Supplementary Table ii.

Protein extraction and western blot analysis

RAW264.7 cells and C2C12 cells were lysed with RIPA lysis buffer (P0013B; Beyotime, China) and phenylmethanesulfonyl fluoride (ST505; Beyotime), and then incubated for 30 minutes on ice. After ultrasonic crushing, the lysate was centrifuged at 14,000 rpm for 30 minutes. The supernatant was taken for protein quantification. RIPA and protein loading buffer (SIANT-BIO, China) were added to set the protein concentration to 3 μg/μl. The samples were boiled for five minutes at 100°C and frozen at -80°C.

A 10% PAGE Gel Fast Preparation Kit (PG212; Epizyme Biomedical Technology, China) was used to prepare electrophoretic gel, 8 μl of protein (24 μg) was added to each lane, electrophoresis was performed at 80 V, and when the Triple Color Prestained Protein Ladder band was clear, the voltage was adjusted to 120 V to continue electrophoresis of different molecular weight proteins for 30 minutes. The membrane was then rotated under a 180 mA current for one hour. The antibodies used were STAT3 (10253-2-AP, rabbit polyclonal; Proteintech, China), β-actin (66009-1-Ig, rabbit polyclonal; Proteintech), matrix metalloproteinase-9 (MMP9) (AF5228, rabbit polyclonal; Affinity, China), cathepsin K (CTSK) (DF6614, rabbit polyclonal; Affinity), tumour necrosis factor receptor-associated protein 1 (TRAP1) (DF7073, rabbit polyclonal; Affinity), FBXO32 (DF7075, rabbit polyclonal; Affinity), Myogenin (DF8273, rabbit polyclonal; Affinity), and TRIM63 (DF7187, rabbit polyclonal; Affinity).

Statistical analysis

All the data were measured at least three times, are expressed as mean and SD, and were statistically analyzed by GraphPad Prism 9 (GraphPad Software). Two-way analysis of variance (ANOVA) was used to analyze the results of reverse transcription-quantitative polymerase chain reaction (RT-qPCR) and western blot analysis, and the comparison between groups was carried out by comparing the results of Šídák's multiple comparisons test.

For the KEGG pathway enrichment analyses, a hypergeometric test was used to assess the statistical significance of gene enrichment in specific pathways, with p-values adjusted for multiple testing using the Benjamini-Hochberg procedure.

Weighted gene co-expression network analysis (WGCNA) was performed to identify modules of co-expressed genes. Soft thresholds were chosen based on scale independence and mean connectivity. Module-clinical relationship heatmaps were used to identify positively correlated modules, and independent-samples *t*-test was employed to determine the statistical significance of these correlations.

Weighted gene co-expression network analysis (WGCNA) was performed on the GSE56814 and GSE1428 datasets to identify modules of co-expressed genes. Soft thresholds were chosen based on scale independence and mean connectivity. Module-clinical relationship heatmaps were used to identify positively correlated modules, and independent-samples *t*-test was employed to determine the statistical significance of these correlations.

Statistical significance was set at $p < 0.05$.

Results

Data download

We paired GSE56814 and GSE1428 as the test queues for WGCNA, and GSE136344 and GSE7158 as the validation queues for differential analysis.

WGCNA

Based on scale independence and mean connectivity, the GSE56814 soft threshold was 20 (R^2 = 0.81) (Figure 1a), and the GSE1428 dataset soft threshold was 16 (R^2 = 0.9) (Figure 1b). In the observation module-clinical relationship heatmap, five modules were identified in GSE56814 species, in which turquoise was the only positive correlation module, and the correlation coefficient was 0.56 (p = 0.002, independent-samples *t*-test), including 1,832 genes (Figures 1c and 1d). Seven modules were identified in GSE1428 species, in which turquoise and brown were positive correlation modules, and the correlation coefficients were 0.62 (p = 0.003) and 0.66 (p = 0.006, both independent-samples *t*-test), respectively, including 2,129 genes (Figures 1c and 1d).

KEGG enrichment analysis of modular intersecting genes

KEGG enrichment analysis of GS1 (defined in the Methods section) (Supplementary Table iii), which consists of 273 overlapping genes from the positive correlation modules of GSE1428 and GSE56814, showed that it was enriched in many pathways, such as 'cysteine and methionine metabolism', 'glutathione metabolism', and 'oxytocin signalling pathway' (Supplementary Figure ba). The oxytocin signalling pathway may be associated with osteoporosis and sarcopenia in the occurrence and development of these two diseases.

Construction of the PPI network and screening of hub genes

We used the STRING database to construct a PPI network of GS1 (Figure 2a). Edge percolation component (EPC) is a method based on network connectivity that calculates the edge penetration component of each node under different thresholds, and evaluates the importance of each node according to its rate of change (Figure 2b). Maximum clique centrality (MCC) is a method based on maximum clique, which calculates the maximum number of cliques to which each node belongs and evaluates the importance of nodes according to their relative position (Figure 2c). Closeness is a method based on the shortest path, which calculates the mean distance from each node to all other nodes and evaluates the importance of the node according to its reciprocal (Figure 2d). Radiality is a method based on the shortest path and network diameter. We used cytoHubba to analyze the common gene expression matrix in the WGCNA positive expression module of osteoporosis and sarcopenia. We found some common genes that were rated as important nodes in all four algorithms. These genes are *ACTB*, *TPI1*, *STAT3*, and *JUN*.

Screening hub genes by machine learning

First, the expression matrix of GS1 in the dataset GSE56814 was extracted, and the *STAT3* and *TRIM22* genes (seed = 4705) (Figure 3a) were obtained by the random forest method. Similarly, the expression matrix of GS1 in the dataset GSE1428 was extracted, and two genes, *STAT3* and *JUN* (seed = 4185) (Figure 3b), were obtained by the random forest method.

The error graph data distribution of the GSE56814 datasets and GSE1428 datasets shows an obvious downward trend, indicating that with the increase in the number of trees, the classification error rate decreases gradually. The data have no outliers. When the number of trees is approximately 280 and 260, the error rate reaches the lowest point and then basically remains stable.

Variable importance maps are a kind of graph used to show the relative importance of different variables in the model. The horizontal axis is the average Gini reduction value, and the vertical axis is the name of the gene (Figures 3c and 3d). By observing the variable importance maps of GSE1428 and GSE56814, we found that the average Gini reduction of the *STAT3* gene was the largest in the two images, so *STAT3* was the most important gene shared by GS1 for the two diseases.

Verification of common genes

KEGG enrichment analysis of the validation GS2 (defined in the Methods section), which contains five overlapping differentially expressed genes (*STAT3*, *JUN*, *TRIM22*, *ALOX5AP*, and *SLC25A6*) from datasets GSE136344 and GSE7158, showed that it was enriched in pathways such as 'thyroid cancer', 'bladder cancer', and 'oxytocin signalling pathway'. Notably, the 'oxytocin signalling pathway' was also enriched in GS1, supporting its potential involvement in the pathogenesis of POMP and sarcopenia (Supplementary Figure bb).

We found the common *STAT3* gene from the genes screened by cytoHubba and random forest, and discovered that there was a significant difference between the disease group and the control group by difference analysis. In the box diagram of GSE7158 as the osteoporosis verification set, the expression of the *STAT3* gene in the disease group was higher than that in the control group (p < 0.001, independent-samples *t*-test) (Figure 4a). In the quadrant map of GSE136433 as the verification set of osteoporosis, the expression of the *STAT3* gene in the disease group was higher than that in the control group (p < 0.001, independent-samples *t*-test) (Figure 4b).

We used *STAT3* as the input gene, GSE7158 and GSE136344 as the verification set, and ROC curves to evaluate the accuracy of the *STAT3* gene in the diagnosis of osteoporosis and sarcopenia. The results show that our model achieves high prediction accuracy on the verification set (GSE7158: AUC 0.923, 95% CI 0.798 to 0.994; GSE136433: AUC 0.917, 95% CI 0.773 to 1.000), indicating that the *STAT3* gene has a very high accuracy in the distinction between osteoporosis and sarcopenia (Figures 4c and 4d).

Results of single-cell analysis

We used reduced-dimensional clustering and uniform manifold approximation and projection (UMAP) visualization to transform thousands of cells in the database into a planar 2D structure, which is convenient for us to observe cell clustering. Then, *STAT3* was extracted to generate the expression density map of the gene in single-cell data. By examining the annotated UMAP map of osteoporosis, we found that all the cells were divided into seven subgroups: macrophages, D14 monocytes, CD16 monocytes, granulocyte-monocyte progenitor cells (GMPs), M2 macrophages, monocytes, and monocyte progenitor cells. *STAT3* was highly expressed in macrophages and GMPs (Figures 5a and 5b). Similarly, ageing muscle cells were divided into eight subgroups: skeletal muscle stem cells (MuSCs), fibro-adipogenic progenitors (FAPs), immune cells, myeloid cells, pericytes, skeletal muscle cells, smooth muscle cells, and

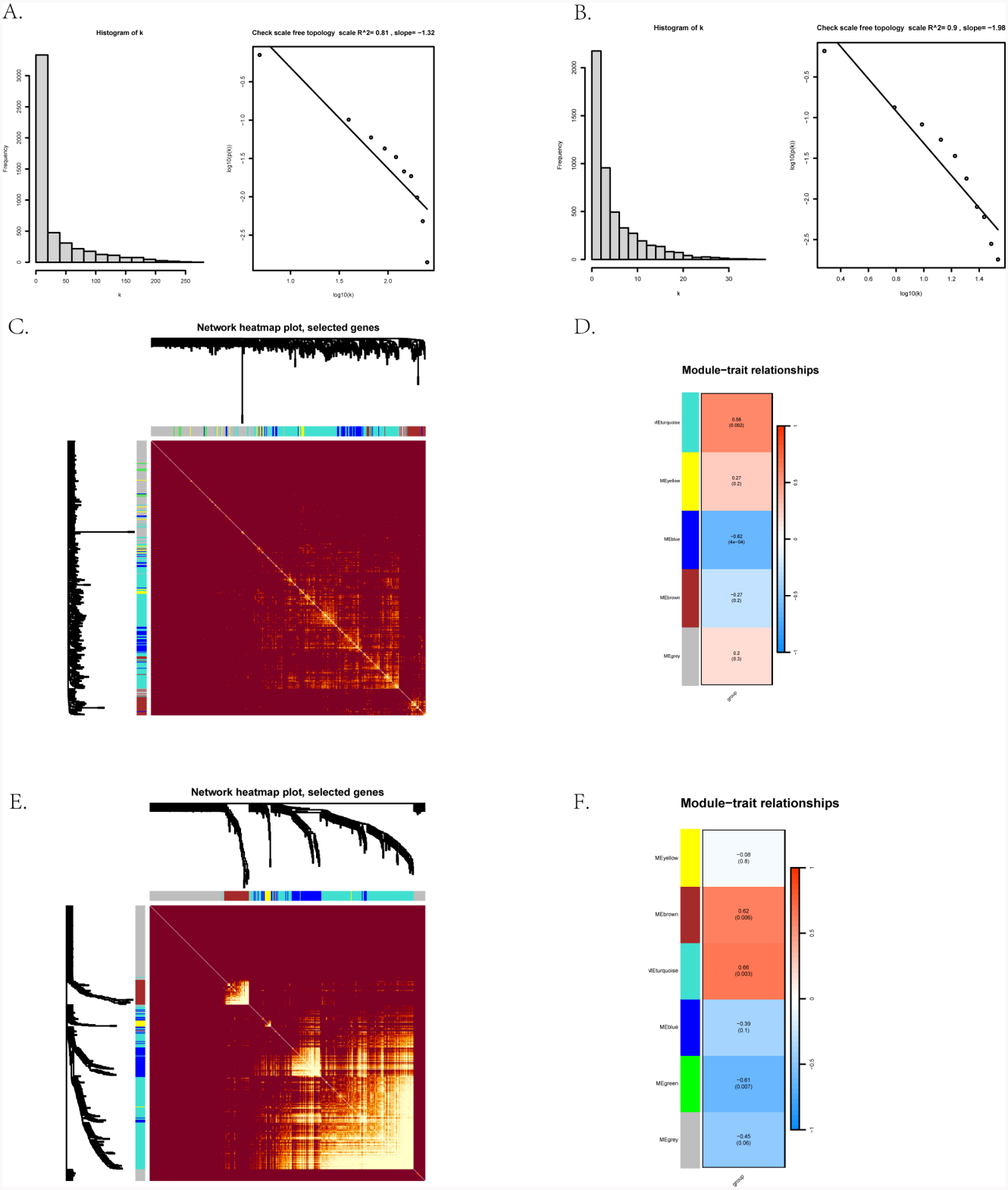

Fig. 1
Weighted gene co-expression network analysis (WGCNA). a) Scale-free network test GSE56814. b) Scale-free network verifies GSE1428. c) Topological overlap matrix (TOM) diagram GSE56814. d) GSE56814 of clinical character heat map. e) TOM diagram GSE1428. f) GSE1428 of clinical character heat map.

stromal cells. *STAT3* was highly expressed in skeletal MuSCs and FAPs (Figures 5c and 5d).

ceRNA network construction

Through the prediction tools miRanda, miRDB, and TargetScan, we built and visualized the *STAT3*-centric miRNA target network. Upregulation of miR-18a-3p has been found to accelerate osteoporosis and may affect immune-mediated

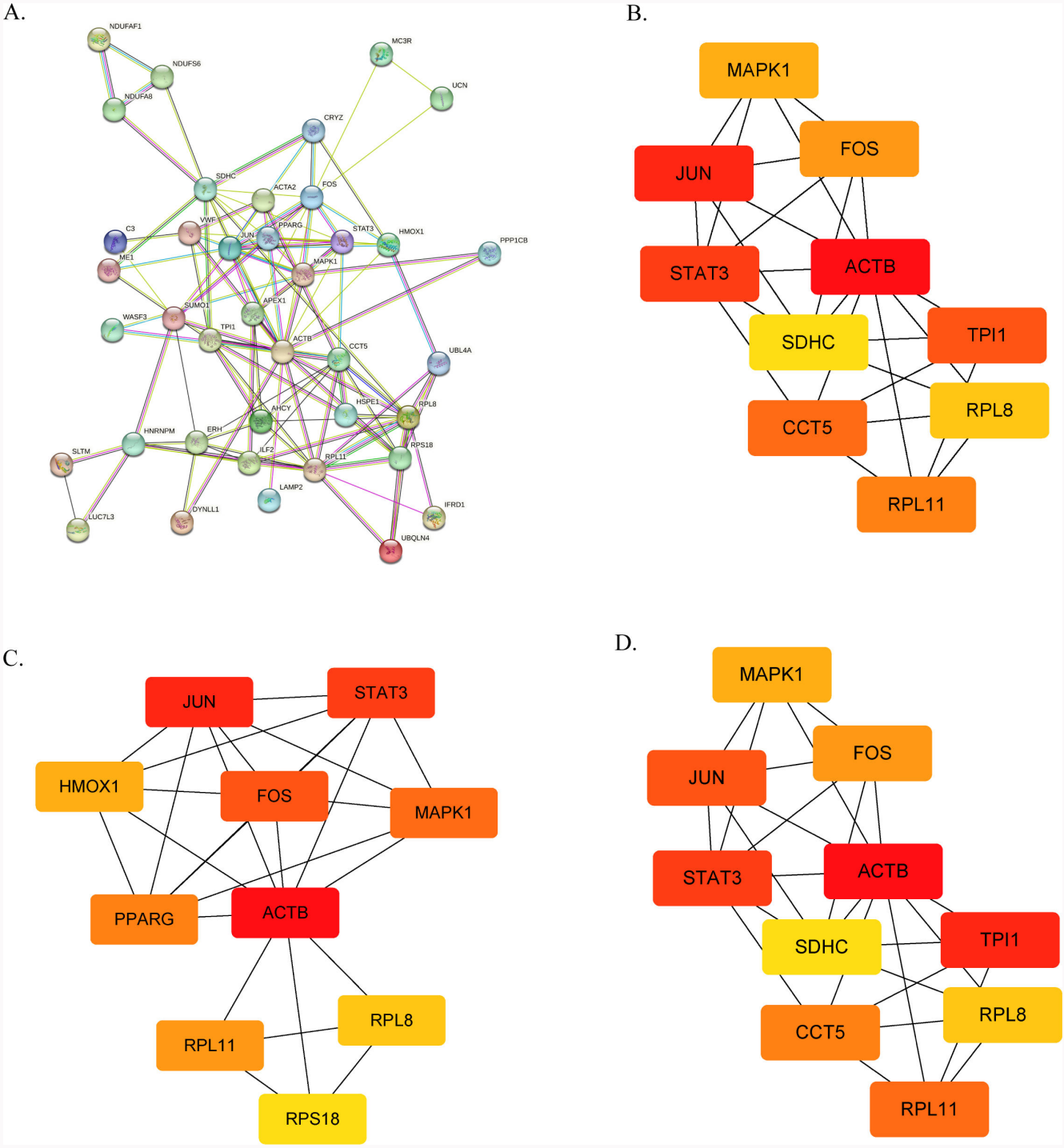

Fig. 2
Protein network construction and hub gene screening. a) Protein-protein interaction network map. b) Hub gene map edge percolation component. c) Hub gene map maximum clique centrality. d) Hub gene map Closeness.

myopathy by inhibiting the GRIA1 gene.[31] However, miR-29a-3p plays a key role in low BMD disease and its drug treatment.[32] In particular, the upregulation of miR-125a-5p can promote osteoclast differentiation, while downregulation has the opposite effect (Figure 6).[33]

STAT3 silencing inhibits osteoclast progenitor cell differentiation and myoblast proliferation

To explore whether the *STAT3* gene can affect bone metabolism and bone formation by affecting osteoclast differentiation of mononuclear macrophages, we used siRNA to perform targeted silencing of the *STAT3* gene in mononuclear macrophages. The RT-qPCR results showed that the messenger RNA (mRNA) expression of osteoclast differentiation-promoting genes MMP9, CTSK, and TRAP1 in the silenced group was significantly lower than that in the control group (Figure 7a). The western blot results were consistent with those of quantitative PCR (qPCR), suggesting that *STAT3* silencing reduced the expression of osteoclast differentiation genes and proteins (Figures 7b and 7c) at both the mRNA and protein

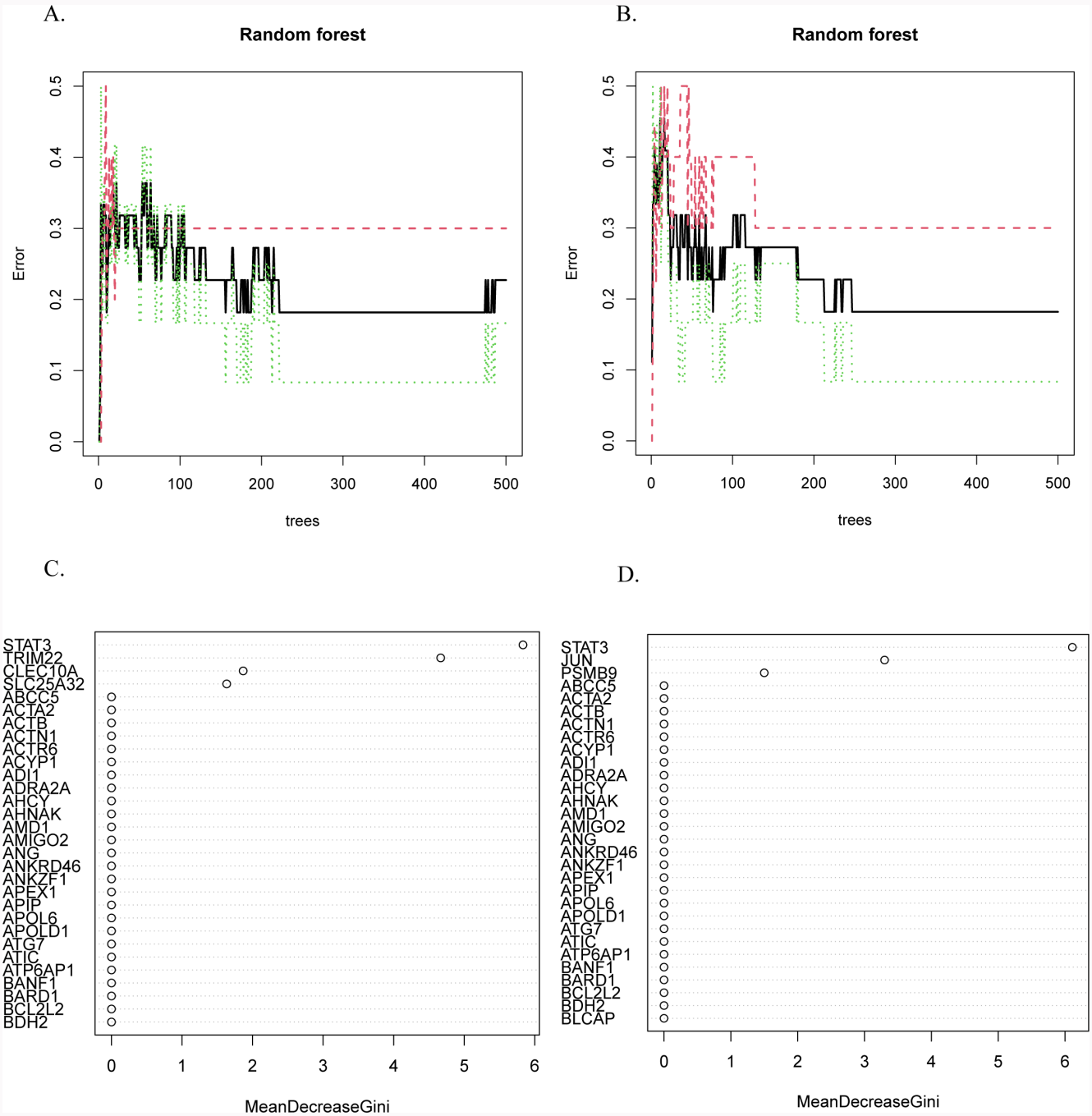

Fig. 3
Machine learning screening hub gene. a) Random forest graph GSE56814. b) Random forest graph GSE1428. c) Random forest graph variable importance GSE56814. d) Random forest graph variable importance GSE1428.

levels. These results suggest that *STAT3* may affect bone metabolism by promoting the differentiation of mononuclear macrophages into osteoclasts, thus promoting bone resorption and reducing bone formation.

We administered the same treatment to myoblasts, and the RT-qPCR and western blot results showed that the expression of muscle atrophy markers *TRIM63* and *FBXO32* in the silenced group was higher than that in the control group, while the expression of muscle marker protein MyoG decreased in the silenced group (Figures 7d to 7f) compared with the control group. These results suggest that silencing of the *STAT3* gene in myoblasts can promote the expression of muscle atrophy markers, and that *STAT3* has a positive effect on myoblast proliferation.

Overexpression of *STAT3* promotes the differentiation of osteoclast progenitor cells but inhibits myoblast proliferation

To further verify the role of *STAT3* in osteoclast progenitor cell differentiation, we used plasmid transfection to overexpress the *STAT3* gene in osteoclasts. In osteoclast progenitor cells, the RT-qPCR and western blot results showed that overexpression of the *STAT3* gene also induced high expression of the osteoclast differentiation genes *MMP9*, *CTSK*, and *TRAP1* (Figures 8a to 8c). These results suggest that the high

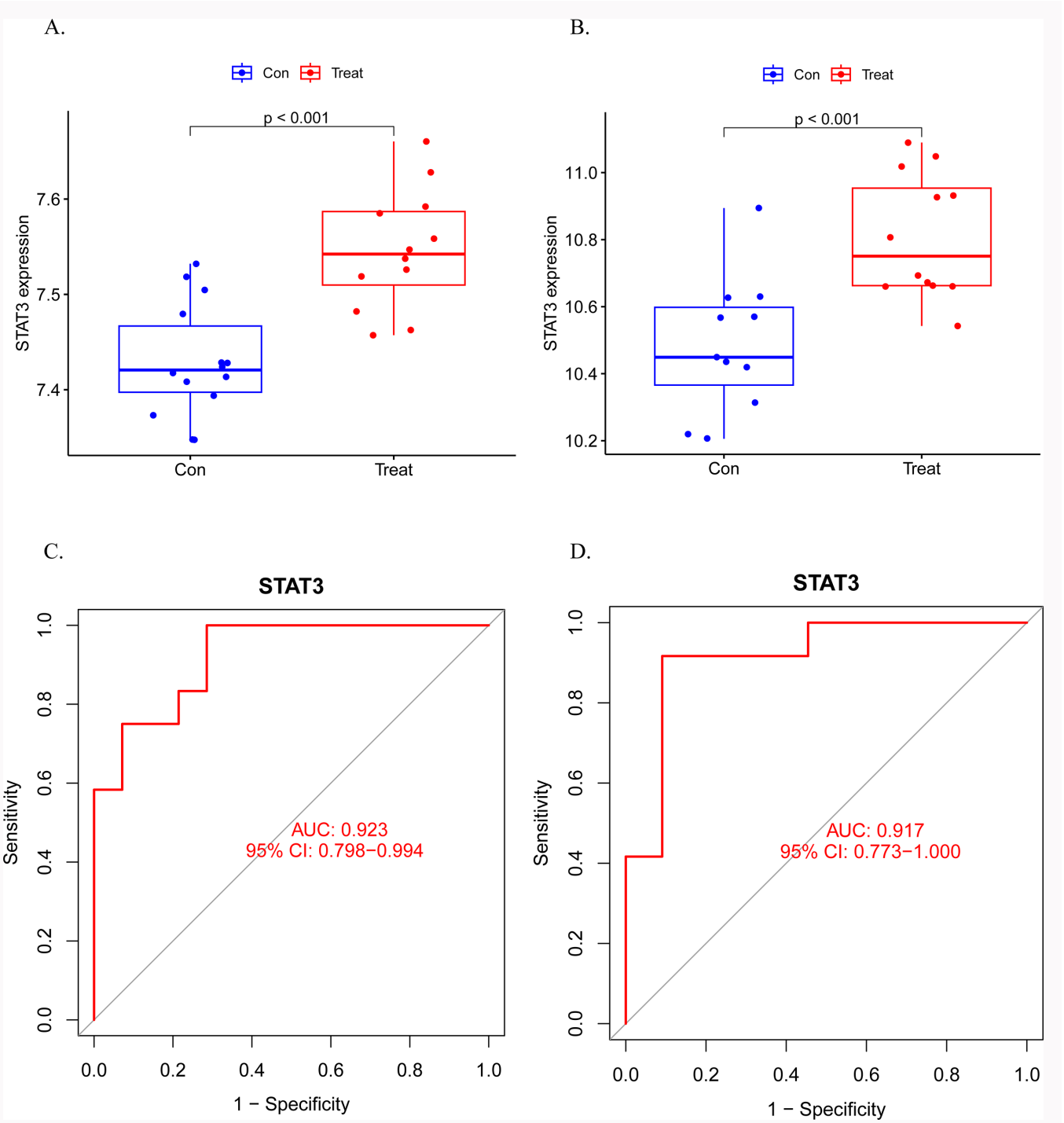

Fig. 4
Verification result. a) Validation set signal transducer and activator of transcription 3 (STAT3) difference analysis chart GSE7158. b) Validation set STAT3 difference analysis chart GSE136433. c) Validation set STAT3 receiver operating characteristic (ROC) curve GSE7158. d) Validation set STAT3 ROC curve GSE136433. All p-values were calculated using independent-samples *t*-test. AUC, area under the curve.

expression of *STAT3* in POMP aggravates the development of POMP by promoting the differentiation of osteoclast precursors into osteoclasts and promoting bone resorption.

Similarly, the *STAT3* gene was overexpressed in myoblasts, and the RT-qPCR and western blot results suggested that overexpression of the *STAT3* gene promoted the expression of muscle atrophy markers *TRIM63* and *FBXO32*, and inhibited the expression of MyoG (Figures 8d to 8f). This finding suggests that the high expression of *STAT3* in sarcopenia may promote the expression of muscular dystrophy factor and lead to muscle mass loss.

Discussion

To find the common ground between the two diseases, we took three steps. First, we found the shared biological pathways and co-expressed genes of the two diseases by analyzing the information in the bulk RNA-seq dataset. Then, the pathways and genes we found were validated in another bulk RNA-seq dataset. We finally confirmed that *STAT3* is a

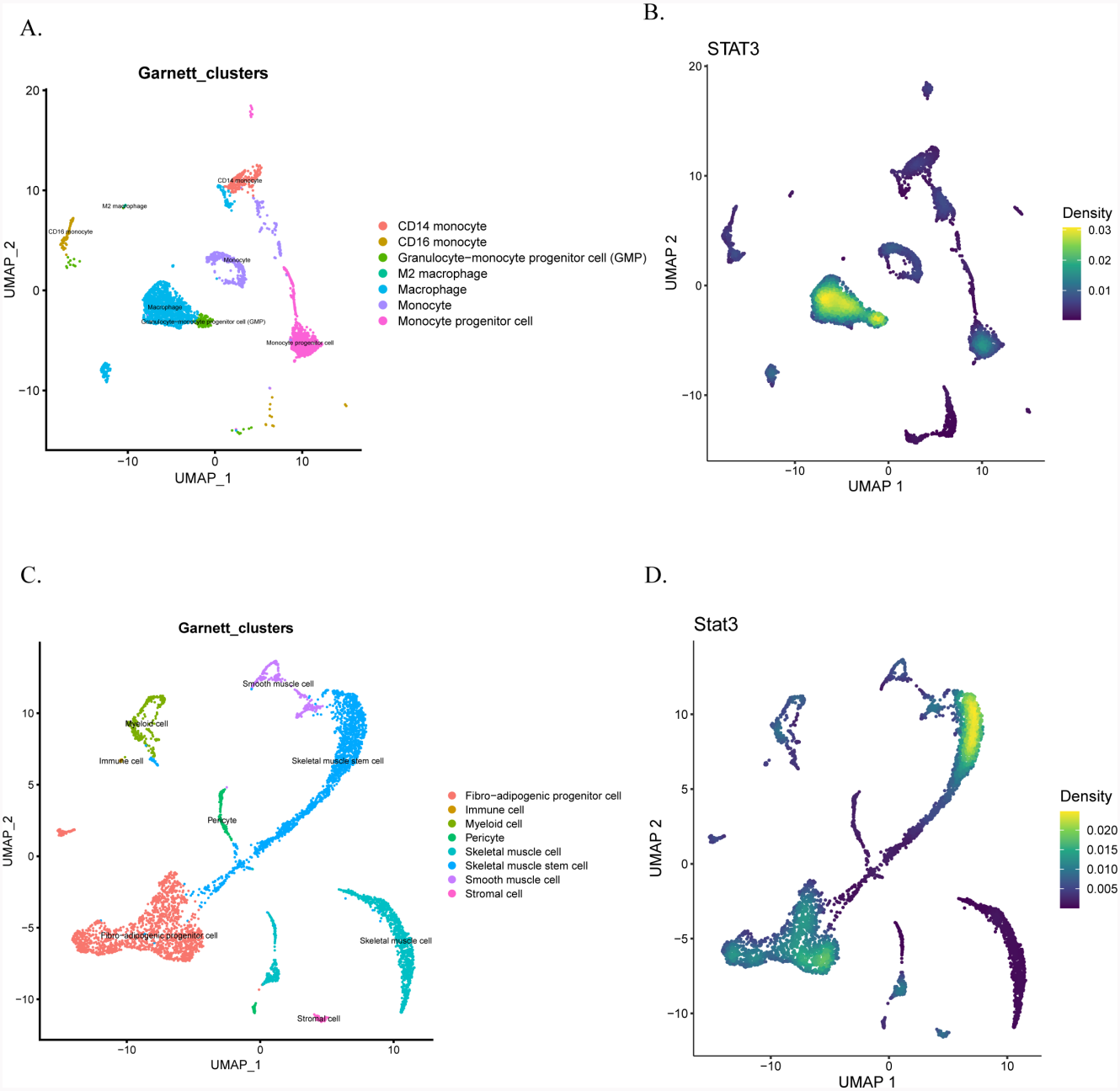

Fig. 5

Single-cell analysis. a) Uniform manifold approximation and projection (UMAP) dimensionality reduction map (osteoporosis). b) Signal transducer and activator of transcription 3 (STAT3) density map (osteoporosis). c) UMAP dimensionality reduction map (sarcopenia). d) STAT3 density map (sarcopenia).

common highly expressed gene in both diseases. To further confirm the distribution of *STAT3* cell subsets in both diseases, we verified the genes at the single-cell level and found that *STAT3* is highly expressed in mononuclear macrophages, MuSCs, and FAPs. Finally, through the construction of a ceRNA network, we found that miRNA-125a-5p is the regulatory factor of *STAT3*. Based on the results of our bioinformatics analysis, experimental results, and existing research progress, *STAT3* is believed to be the key co-pathogenic gene of POMP and sarcopenia. Designing drugs targeting *STAT3* itself or its regulatory factor might have a better therapeutic effect on both diseases than treating one of them alone.

STAT3 is a signal sensor and transcriptional activator that plays an important role in the regulation of cell proliferation, apoptosis, and differentiation.[34] Yang et al[35] noted that the bone mass of mice with osteoclast-specific *STAT3* deficiency was significantly higher than that of the control group. Some scholars have found that IL-6 causes septicaemia-induced muscle mass loss through the gp130/JAK2/STAT3 pathway, and muscle mass loss is alleviated after the use of this channel inhibitor.[36] The pathogenesis of osteoporosis combined with sarcopenia is not clear, but our study found that STAT3 may be a common pathogenic target of both diseases and play a very important role in both diseases.

RANKL/RANK is an important regulatory axis of muscle and bone metabolism. RANKL is recognized as an important molecule that affects osteoclast differentiation, together with

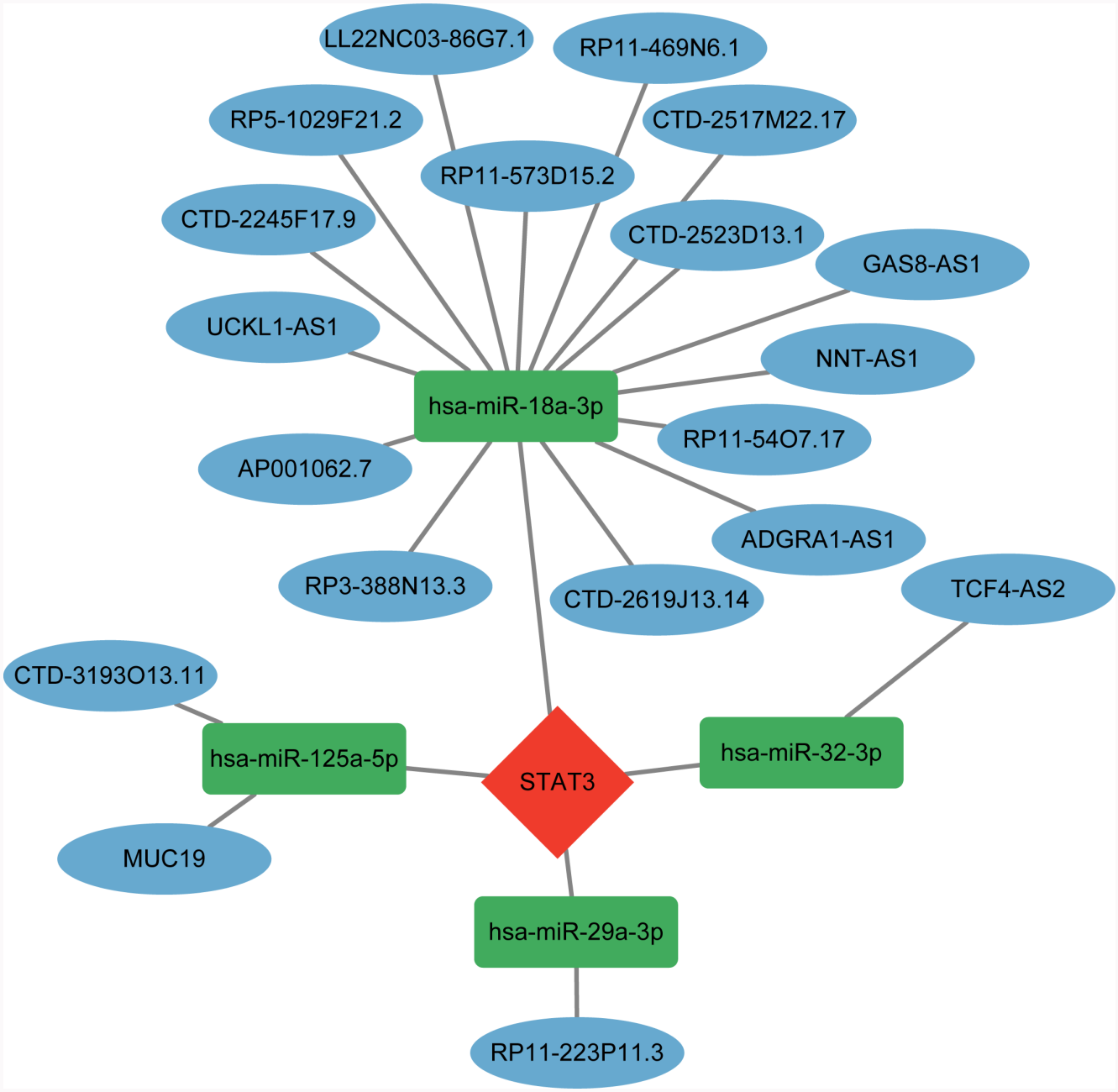

Fig. 6
Competing endogenous RNA (ceRNA) network diagram. miR, microRNA; STAT3, signal transducer and activator of transcription 3.

macrophage colony-stimulating factor (M-CSF).[37] STAT3 is an important activation signal molecule of the RANKL/RANK pathway. It has been proven that the activation of the JAK2/STAT3 axis by interleukin (IL)-6 to promote the expression of RANKL is an important step in osteoclast differentiation of mononuclear macrophages.[38] Overactivated osteoclasts lead to bone resorption, resulting in osteopenia and osteoporosis.[39] Furthermore, our KEGG enrichment analysis also highlighted the oxytocin signalling pathway as over-represented in both the gene modules related to POMP and sarcopenia. Oxytocin has been reported to have a dual effect on bone metabolism. On one hand, it promotes osteoblast differentiation and function, leading to increased bone formation.[40–43] Oxytocin stimulates the differentiation of osteoblasts and upregulates the expression of genes involved in osteoblast differentiation, resulting in enhanced bone mineralization and formation.[42,43] On the other hand, oxytocin has a complex effect on osteoclasts. It can stimulate osteoclast formation, both directly by activating specific signalling pathways and indirectly by upregulating RANKL production by osteoblasts. However, oxytocin also inhibits bone resorption activity of mature osteoclasts by triggering calcium release and nitric oxide synthesis.[43] This suggests that oxytocin plays a crucial role in regulating the balance between bone formation and resorption. Dysregulation of oxytocin signalling may contribute to the development of osteoporosis by disrupting this delicate balance. The involvement of the oxytocin pathway in both POMP and sarcopenia gene modules indicates its potential as a molecular link between muscle and bone pathologies, which warrants further investigation.

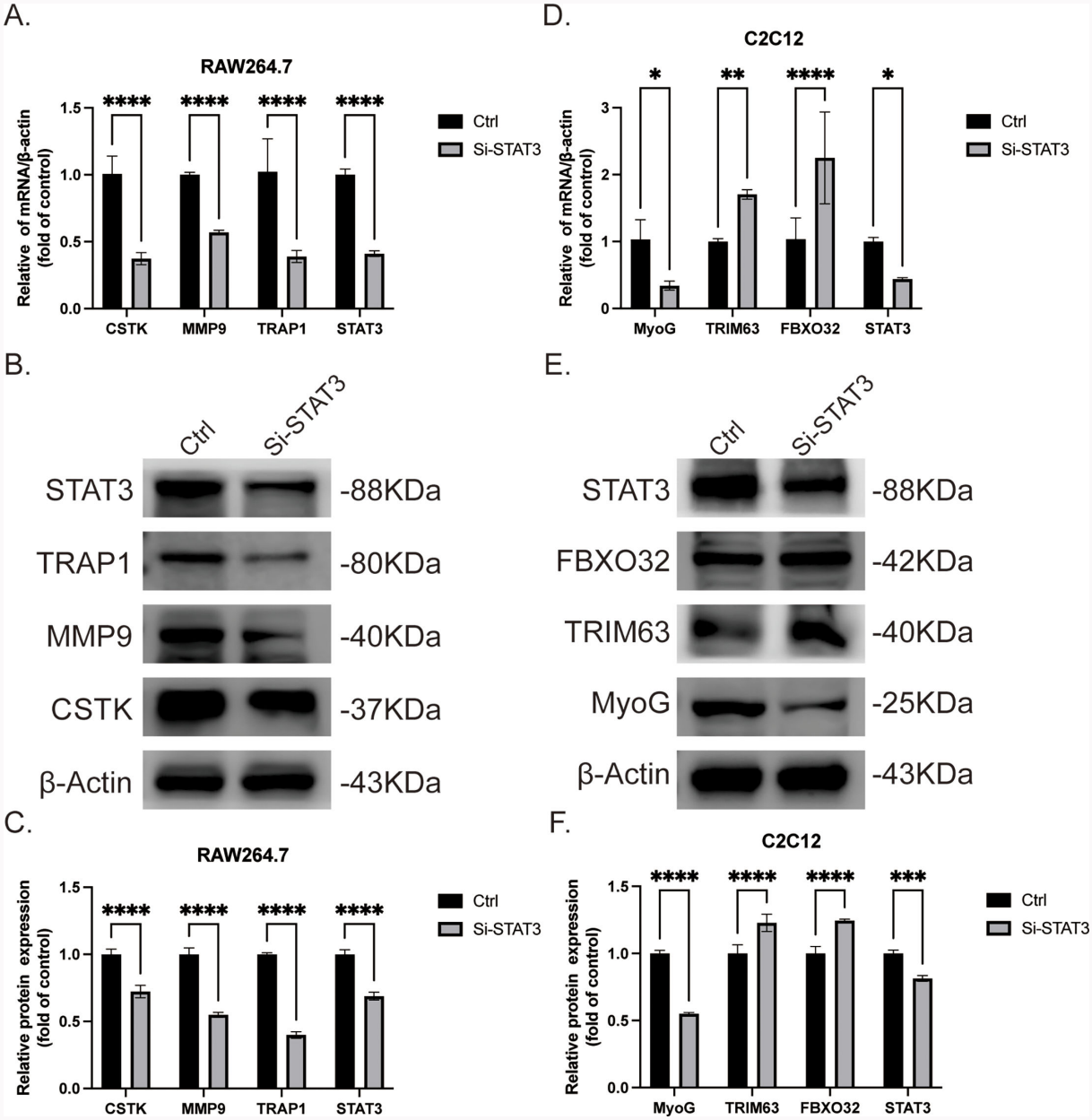

Fig. 7

RAW264.7 osteoclast progenitor cells and C2C12 myoblasts were transfected with signal transducer and activator of transcription 3 (STAT3) small interfering RNA (siRNA). a) The expression of STAT3 and matrix metalloproteinase-9 (MMP9) was determined by reverse transcription-quantitative polymerase chain reaction (RT-qPCR). STAT3 messenger RNA (mRNA) in the treatment group was significantly decreased by siRNA, and MMP9 mRNA was also significantly lower than that in the control group. b) Western blot expressing protein in osteoclast progenitor cells. After 48 hours of siRNA silencing, the expression of STAT3 and MMP9 was significantly decreased. c) The gray value of western blot of osteoclast precursor cells was statistically analyzed. d) The expression of STAT3 and TRIM63 was determined by RT-qPCR. In the treatment group, STAT3 mRNA was significantly decreased by siRNA, while MMP9 mRNA was significantly higher than that in the control group. e) Western blot expressing proteins in myoblasts. After 48 hours of siRNA silencing, the expression of STAT3 was significantly decreased and the expression of Trim63 was significantly increased. f) The western blot gray values of myoblasts were statistically analyzed. **$p < 0.01$, ***$p < 0.001$, ****$p < 0.0001$ (Šídák's multiple comparisons test). The number of samples in each set of experimental data is 3. CSTK, cytokine suppressive anti-inflammatory kinase; Ctrl, control; FBXO32, F-box only protein 32; MyoG, myogenin; STAT3, signal transducer and activator of transcription 3; si-STAT3, small interfering RNA targeting STAT3; TNF, tumour necrosis factor, TRAP1, TNF receptor-associated protein 1; TRIM63, tripartite motif containing 63.

Through single-cell analysis of the POMP dataset, we determined that the *STAT3* gene was highly expressed in mononuclear macrophages, while overexpression and knockdown of STAT3 influenced the activity of macrophages via MMP9, CTSK, and TRAP1. Therefore, we speculate that STAT3 is involved in osteoporosis by promoting osteoclast differentiation of macrophages.

STAT3 also plays an irreplaceable role in sarcopenia due to various causes, including ageing, physical, poor nutrition, chronic diseases, hormonal changes, inflammation, oxidative stress, neurodegenerative processes, genetics, and medication. However, there are contradictions about the role of *STAT3* in muscle. Some studies have found that STAT3 can promote muscle regeneration by activating satellite cells, and the activation of STAT3 can also directly promote the function of

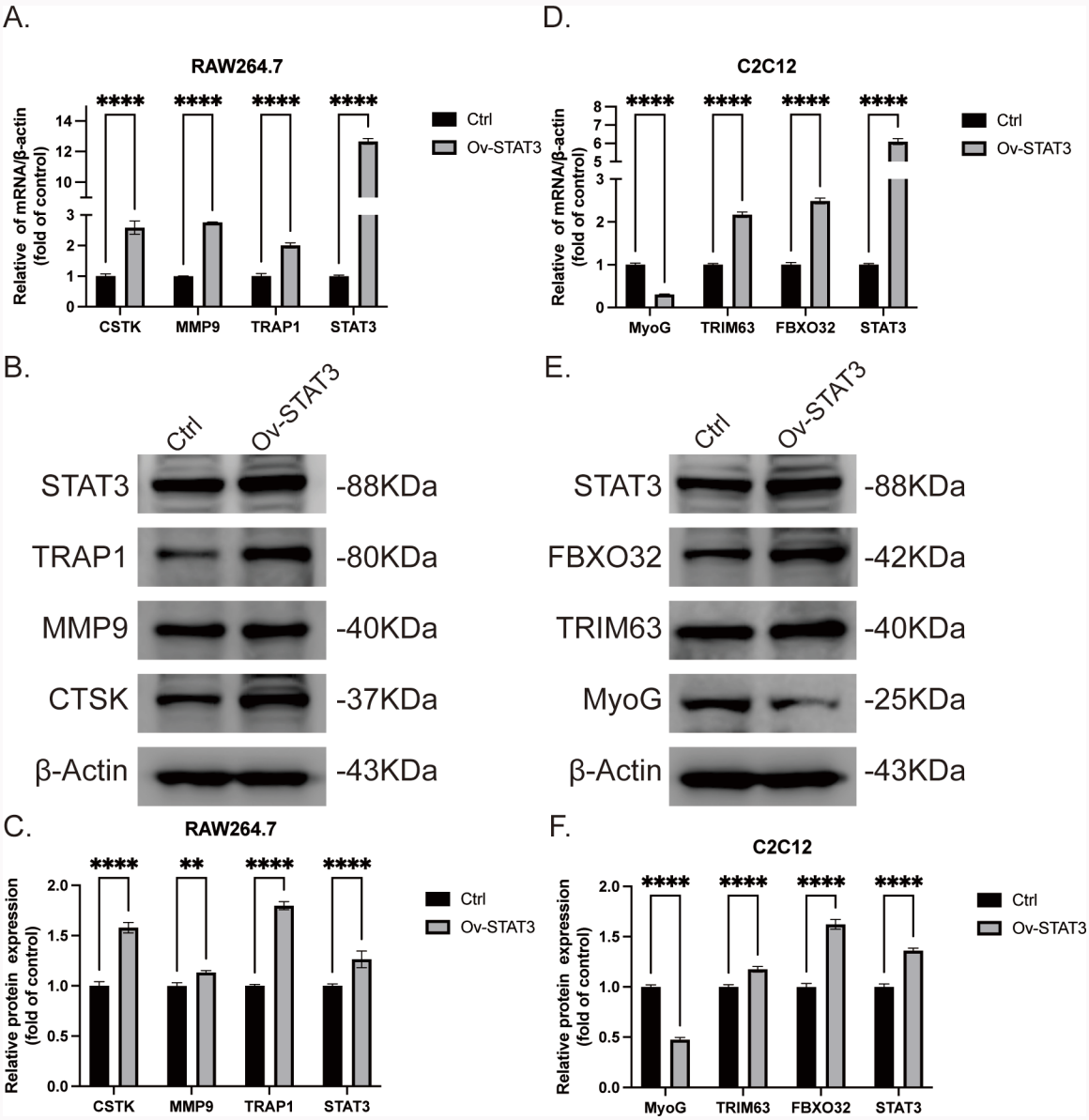

Fig. 8

Plasmid was transfected into RAW264.7 osteoclast progenitor cells and C2C12 myoblasts. a) The expression of signal transducer and activator of transcription 3 (STAT3) and matrix metalloproteinase-9 (MMP9) was determined by reverse transcription-quantitative polymerase chain reaction (RT-qPCR). The genes of STAT3 and MMP9 in the treatment group were significantly overexpressed by the plasmid compared with the control group. b) Western blot of protein expressed by osteoclast progenitor cells; 48 hours after overexpression of plasmid, the expression of STAT3 and MMP9 protein increased. c) Statistical analysis of western blot gray value of osteoclast progenitor cells. d) The expression of STAT3 and TRIM63 was detected by RT-qPCR. The genes of STAT3 and TRIM63 in the treatment group were significantly overexpressed by the plasmid compared with the control group. e) Western blot of protein expressed by myoblasts; 48 hours after overexpression of plasmid, the expression of STAT3 and TRIM63 protein increased. f) Statistical analysis of western blot gray value of myoblasts. **p < 0.01, ***p < 0.001, ****p < 0.0001 (Šídák's multiple comparisons test). The number of samples in each set of experimental data is 3. CSTK, cytokine suppressive anti-inflammatory kinase; Ctrl, control; FBXO32, F-box only protein 32; MyoG, myogenin; STAT3, Ov-STAT3, overexpression of STAT3; STAT3, signal transducer and activator of transcription 3; TNF, tumour necrosis factor, TRAP1, TNF receptor-associated protein 1; TRIM63, tripartite motif containing 63.

mitochondria in skeletal MuSCs.[44,45] These studies have shown that STAT3 plays a positive role in muscle mass and repair by acting on muscle cells or muscle helper cells. Moreover, a large number of studies have published different views, such as the belief that the activation of the JAK2/STAT3 pathway mediated by IL-6 can lead to muscle atrophy, and that STAT3 inhibition can reduce muscle atrophy caused by cancer cachexia.[46] Excessive activation of STAT3 in muscle cells in diabetes or chronic kidney disease can lead to muscle loss, and targeted knockout of STAT3 or inhibition of STAT3 expression in muscle can improve muscle quality.[47] We confirmed the high expression of the *STAT3* gene in skeletal MuSCs and FAPs in the disease group by single-cell analysis, suggesting that *STAT3* may be closely related to sarcopenia. We silenced and overexpressed *STAT3* in myoblasts, the muscle atrophy markers *TRIM63* and *FBXO32* increased, and the expression of MyoG decreased. This phenomenon suggests that there is a certain expression range of STAT3, and too high or too low levels of STAT3 will affect the physiological function of muscle.

Given these two completely different viewpoints, we speculate that STAT3 will have different effects when the muscles are in different states. When the body is in a steady

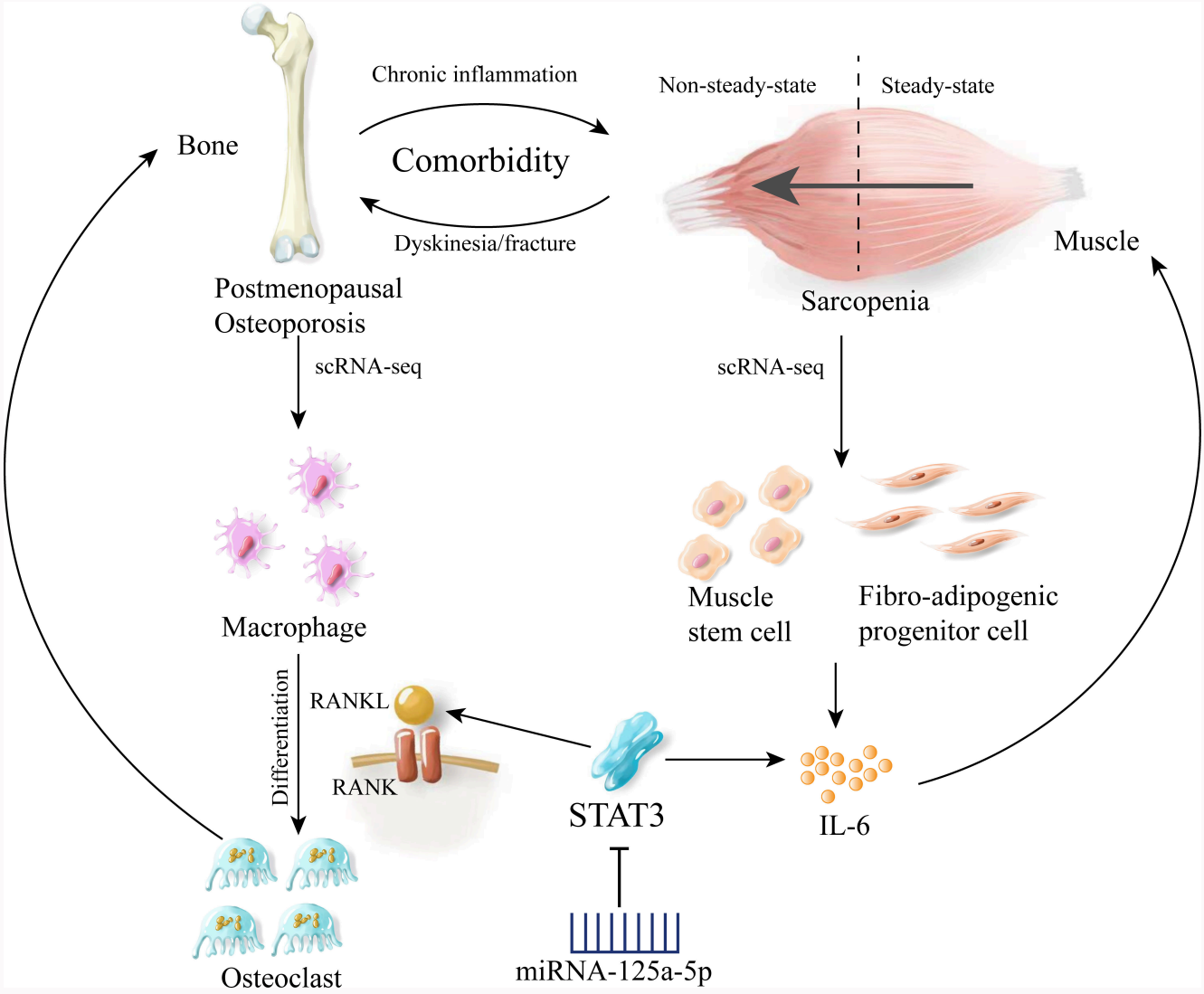

Fig. 9

Proposed molecular mechanisms linking postmenopausal osteoporosis (POMP) and sarcopenia. Chronic inflammation and comorbidity lead to a bidirectional interaction between bone and muscle, known as the bone-muscle axis. In POMP, single-cell RNA sequencing (scRNA-seq) analysis reveals high signal transducer and activator of transcription 3 (STAT3) expression in macrophages, which activates the RANKL/RANK pathway and promotes osteoclast differentiation, leading to increased bone resorption and dyskinesia/fracture. In sarcopenia, scRNA-seq analysis shows elevated STAT3 expression in muscle stem cells and fibro-adipogenic progenitors (FAPs). Abnormally activated FAPs overexpress STAT3 and secrete interleukin (IL)-6, resulting in muscle atrophy and fibrosis. The competing endogenous RNA (ceRNA) network analysis identifies microRNA (miRNA)-125a-5p as a potential regulator of STAT3, suggesting its role in modulating the pathogenesis of both diseases. The comorbidity and interaction between POMP and sarcopenia exacerbate each other, leading to a non-steady-state condition. Targeting the shared molecular pathways, such as the STAT3/miRNA-125a-5p axis, may provide a novel therapeutic strategy for managing these age-related musculoskeletal disorders.

state, STAT3, as an important signalling molecule, is directly involved in muscle synthesis and repair. Under unstable conditions such as chronic injury and inflammation caused by disease, as well as insulin resistance, excessive activation of STAT3 leads to muscle atrophy.[36] FAPs are activated when muscle injury occurs and interact with MuSCs to promote muscle repair. A 2018 study clarified in detail that FAPs continue to activate STAT3 and secrete a large amount of IL-6 in muscular atrophy models, resulting in muscle atrophy and fibrosis, which can be alleviated in mice with STAT3 signal knockout in FAPs.[48]

Bone and muscle are interrelated, and the interaction between them is called the bone-muscle axis. Although sarcopenia and osteoporosis were initially considered to be separate diseases, recent studies have shown that bones and muscles are spatially and metabolically connected.[49] This interaction, known as skeletal and muscular comorbidity, indicates a synergistic effect between low BMD and muscle atrophy and low function (Figure 9).[50] Osteoporosis is closely related to chronic inflammation and oxidative damage. In the case of osteoporosis, the bone microenvironment changes, which may affect adjacent muscle tissue. Our results show that macrophages highly express *STAT3* during the pathogenesis of osteoporosis, which in turn activates the RANK/RANKL pathway, promotes bone resorption, and aggravates osteoporosis. This aggravation of osteoporosis may further exacerbate chronic inflammation, creating a vicious circle. A chronic inflammatory environment can damage not only bone tissue but also muscle cells. In this environment, FAPs and MuSCs may be activated in an unstable state. Abnormally activated

FAPs overexpress *STAT3* and secrete a large amount of IL-6, which leads to muscle atrophy and fibrosis and further reduces the muscle mass of patients.[48] Sarcopenia not only affects the ability to exercise of patients, but also may have a negative impact on bone health. Muscle is not only a motor organ but also an important endocrine organ. Muscles can secrete various cytokines (such as irisin and insulin-like growth factor 1 (IGF-1)) to regulate bone homeostasis.[9] In the state of muscle atrophy, the secretion of muscle factors decreases, which aggravates osteoporosis.[51] Moreover, mechanical stimulation between muscle and bone is a key factor in maintaining BMD.[52] When muscle mass decreases, mechanical stimulation to bones also decreases, which may lead to a decrease in BMD. In addition, sarcopenia may lead to increased chronic inflammation and oxidative stress, both of which are associated with bone metabolic disorders and increased bone resorption.[53]

As mentioned above, osteoporosis and sarcopenia exacerbate each other, so treating one of these diseases alone cannot break this vicious circle, and it is necessary to find a target to treat both diseases. Our study found a common therapeutic target, *STAT3*, but how to regulate the expression of this key gene is still a problem. Therefore, we identified the upstream regulatory factor of *STAT3*, *miRNA-125a-5p*, by constructing a ceRNA network. *miRNA-125a-5p/STAT3* plays a regulatory role in the occurrence and development of osteoporosis and sarcopenia. Previous studies have shown that *miR-125a-5p* enhances the level of autophagy by targeting STAT3.[54] This finding confirms that *miRNA-125a-5p* can regulate pathophysiological activity by targeting STAT3. Therefore, we speculate that *miRNA-125a-5p* mediates the expression of *RANKL* through targeted regulation of STAT3 in macrophages and affects the process of osteoporosis. Moreover, through targeted regulation of STAT3 in MuSCs and FAPs, it mediates the IL-6 signalling pathway and affects the progression of sarcopenia. Therefore, *miRNA-125a-5p*, as an important regulator of STAT3, may be a potential therapeutic target for the development of drugs to treat both osteoporosis and sarcopenia.

Comorbidity is characterized by a common underlying mechanism and the need for co-treatments.[55] There is a common target for concurrent treatment of comorbid diseases, which has implications for the prevention and treatment of disorders. Osteoporosis and sarcopenia are also comorbidities in bones and muscles, and effective therapeutic approaches are lacking. In this study, *miRNA-125a-5p* was identified as a potential concurrent treatment for osteoporosis and sarcopenia via interaction with the mRNA of *STAT3*. These findings provide a more comprehensive perspective and help us to understand the complex relationship between osteoporosis and sarcopenia. Future research should focus on the common management and treatment of common diseases, while medications focusing on common targets of the comorbidity of osteoporosis and sarcopenia may bring about better therapeutic effects.

Supplementary material

Figure a provides an overall research and design flowchart. Table i lists datasets related to sarcopenia and osteoporosis, including sample sizes for control and disease groups, obtained from the Gene Expression Omnibus (GEO) database. Detailed RNA extraction and quantitative polymerase chain reaction (qPCR) methodologies are described, with specific primer sequences listed in Table ii. Additionally, Kyoto Encyclopedia of Genes and Genomes (KEGG) enrichment analysis results for gene set 1 (GS1) are presented in Table iii, highlighting key pathways such as cysteine and methionine metabolism, and the oxytocin signalling pathway, further explored in Figures ba and bb.

References

1. **Chen K**, **Lv Z-T**, **Cheng P**, **et al**. Boldine ameliorates estrogen deficiency-induced bone loss via inhibiting bone resorption. *Front Pharmacol*. 2018;9:1046.
2. **Fielding RA**, **Vellas B**, **Evans WJ**, **et al**. Sarcopenia: an undiagnosed condition in older adults. Current consensus definition: prevalence, etiology, and consequences. International working group on sarcopenia. *J Am Med Dir Assoc*. 2011;12(4):249–256.
3. **Buckinx F**, **Landi F**, **Cesari M**, **et al**. Pitfalls in the measurement of muscle mass: a need for a reference standard. *J Cachexia Sarcopenia Muscle*. 2018;9(2):269–278.
4. **Hernández-Álvarez D**, **Mena-Montes B**, **Toledo-Pérez R**, **et al**. Long-term moderate exercise combined with metformin treatment induces an hormetic response that prevents strength and muscle mass loss in old female wistar rats. *Oxid Med Cell Longev*. 2019;2019:3428543.
5. **Coin A**, **Perissinotto E**, **Enzi G**, **et al**. Predictors of low bone mineral density in the elderly: the role of dietary intake, nutritional status and sarcopenia. *Eur J Clin Nutr*. 2008;62(6):802–809.
6. **Ellman R**, **Spatz J**, **Cloutier A**, **Palme R**, **Christiansen BA**, **Bouxsein ML**. Partial reductions in mechanical loading yield proportional changes in bone density, bone architecture, and muscle mass. *J Bone Miner Res*. 2013;28(4):875–885.
7. **Batsis JA**, **Villareal DT**. Sarcopenic obesity in older adults: aetiology, epidemiology and treatment strategies. *Nat Rev Endocrinol*. 2018;14(9):513–537.
8. **Edwards MH**, **Dennison EM**, **Aihie Sayer A**, **Fielding R**, **Cooper C**. Osteoporosis and sarcopenia in older age. *Bone*. 2015;80:126–130.
9. **Greco EA**, **Pietschmann P**, **Migliaccio S**. Osteoporosis and sarcopenia increase frailty syndrome in the elderly. *Front Endocrinol (Lausanne)*. 2019;10:255.
10. **Dufresne SS**, **Dumont NA**, **Boulanger-Piette A**, **et al**. Muscle RANK is a key regulator of Ca2+ storage, SERCA activity, and function of fast-twitch skeletal muscles. *Am J Physiol Cell Physiol*. 2016;310(8):C663–72.
11. **Roux C**, **Briot K**. How long should we treat? *Osteoporos Int*. 2014;25(6):1659–1666.
12. **Hsu W-B**, **Lin S-J**, **Hung J-S**, **et al**. Effect of resistance training on satellite cells in old mice - a transcriptome study: implications for sarcopenia. *Bone Joint Res*. 2022;11(2):121–133.
13. **Colaianni G**, **Cinti S**, **Colucci S**, **Grano M**. Irisin and musculoskeletal health. *Ann N Y Acad Sci*. 2017;1402(1):5–9.
14. **Abe S**, **Kashii M**, **Shimada T**, **et al**. Relationship between distal radius fracture severity and 25-hydroxyvitamin-D level among perimenopausal and postmenopausal women. *Bone Jt Open*. 2022;3(3):261–267.
15. **Gautier L**, **Cope L**, **Bolstad BM**, **Irizarry RA**. affy--analysis of Affymetrix GeneChip data at the probe level. *Bioinformatics*. 2004;20(3):307–315.
16. **Du P**, **Kibbe WA**, **Lin SM**. lumi: a pipeline for processing Illumina microarray. *Bioinformatics*. 2008;24(13):1547–1548.
17. **Leek JT**, **Johnson WE**, **Parker HS**, **Jaffe AE**, **Storey JD**. The sva package for removing batch effects and other unwanted variation in high-throughput experiments. *Bioinformatics*. 2012;28(6):882–883.
18. **Yu G**, **Wang L-G**, **Han Y**, **He Q-Y**. clusterProfiler: an R package for comparing biological themes among gene clusters. *OMICS*. 2012;16(5):284–287.
19. **Yuan W**, **Yang M**, **Zhu Y**. Development and validation of a gene signature predicting the risk of postmenopausal osteoporosis. *Bone Joint Res*. 2022;11(8):548–560.
20. **Xiang C**, **Liao Y**, **Chen Z**, **et al**. Network pharmacology and molecular docking to elucidate the potential mechanism of ligusticum chuanxiong against osteoarthritis. *Front Pharmacol*. 2022;13:854215.
21. **No authors listed**. STRING: functional protein association networks. 2023. https://string-db.org/ (date last accessed 29 July 2024).

22. **Chin C-H**, **Chen S-H**, **Wu H-H**, **Ho C-W**, **Ko M-T**, **Lin C-Y**. cytoHubba: identifying hub objects and sub-networks from complex interactome. *BMC Syst Biol*. 2014;8 Suppl 4(Suppl 4):S11.
23. **Hu J**, **Szymczak S**. A review on longitudinal data analysis with random forest. *Brief Bioinform*. 2023;24(2):bbad002.
24. **Ritchie ME**, **Phipson B**, **Wu D**, **et al**. limma powers differential expression analyses for RNA-sequencing and microarray studies. *Nucleic Acids Res*. 2015;43(7):e47.
25. **Robin X**, **Turck N**, **Hainard A**, **et al**. pROC: an open-source package for R and S+ to analyze and compare ROC curves. *BMC Bioinformatics*. 2011;12:77.
26. **Hao Y**, **Hao S**, **Andersen-Nissen E**, **et al**. Integrated analysis of multimodal single-cell data. *Cell*. 2021;184(13):3573–3587.
27. **Korsunsky I**, **Millard N**, **Fan J**, **et al**. Fast, sensitive and accurate integration of single-cell data with Harmony. *Nat Methods*. 2019;16(12):1289–1296.
28. **Min H**, **Yoon S**. Got target? Computational methods for microRNA target prediction and their extension. *Exp Mol Med*. 2010;42(4):233–244.
29. **Pliner HA**, **Shendure J**, **Trapnell C**. Supervised classification enables rapid annotation of cell atlases. *Nat Methods*. 2019;16(10):983–986.
30. **Alquicira-Hernandez J**, **Powell JE**. Nebulosa recovers single-cell gene expression signals by kernel density estimation. *Bioinformatics*. 2021;37(16):2485–2487.
31. **Zhao M**, **Dong J**, **Liao Y**, **et al**. MicroRNA miR-18a-3p promotes osteoporosis and possibly contributes to spinal fracture by inhibiting the glutamate AMPA receptor subunit 1 gene (GRIA1). *Bioengineered*. 2022;13(1):370–382.
32. **Kyei B**, **Odame E**, **Li L**, **et al**. Knockdown of CDR1as decreases differentiation of goat skeletal muscle satellite cells via upregulating miR-27a-3p to inhibit ANGPT1. *Genes (Basel)*. 2022;13(4):663.
33. **Sun L**, **Lian JX**, **Meng S**. MiR-125a-5p promotes osteoclastogenesis by targeting TNFRSF1B. *Cell Mol Biol Lett*. 2019;24:23.
34. **Lee SW**, **Ahn YY**, **Kim YS**, **et al**. The immunohistochemical expression of STAT3, Bcl-xL, and MMP-2 proteins in colon adenoma and adenocarcinoma. *Gut Liver*. 2012;6(1):45–51.
35. **Yang Y**, **Chung MR**, **Zhou S**, **et al**. STAT3 controls osteoclast differentiation and bone homeostasis by regulating NFATc1 transcription. *J Biol Chem*. 2019;294(42):15395–15407.
36. **Zanders L**, **Kny M**, **Hahn A**, **et al**. Sepsis induces interleukin 6, gp130/JAK2/STAT3, and muscle wasting. *J Cachexia Sarcopenia Muscle*. 2022;13(1):713–727.
37. **Kim MH**, **Choi LY**, **Chung JY**, **Kim E-J**, **Yang WM**. Auraptene ameliorates osteoporosis by inhibiting RANKL/NFATc1 pathway-mediated bone resorption based on network pharmacology and experimental evaluation. *Bone Joint Res*. 2022;11(5):304–316.
38. **Harmer D**, **Falank C**, **Reagan MR**. Interleukin-6 interweaves the bone marrow microenvironment, bone loss, and multiple myeloma. *Front Endocrinol (Lausanne)*. 2018;9:788.
39. **Wang X**, **Jiang W**, **Pan K**, **Tao L**, **Zhu Y**. Melatonin induces RAW264.7 cell apoptosis via the BMAL1/ROS/MAPK-p38 pathway to improve postmenopausal osteoporosis. *Bone Joint Res*. 2023;12(11):677–690.
40. **Feixiang L**, **Yanchen F**, **Xiang L**, **et al**. The mechanism of oxytocin and its receptors in regulating cells in bone metabolism. *Front Pharmacol*. 2023;14:1171732.
41. **Breuil V**, **Trojani M-C**, **Ez-Zoubir A**. Oxytocin and bone: review and perspectives. *Int J Mol Sci*. 2021;22(16):8551.
42. **Colaianni G**, **Sun L**, **Zaidi M**, **Zallone A**. The "love hormone" oxytocin regulates the loss and gain of the fat-bone relationship. *Front Endocrinol (Lausanne)*. 2015;6:79.
43. **Colaianni G**, **Tamma R**, **Di Benedetto A**, **et al**. The oxytocin-bone axis. *J Neuroendocrinol*. 2014;26(2):53–57.
44. **Blankenbach KV**, **Schwalm S**, **Pfeilschifter J**, **Meyer Zu Heringdorf D**. Sphingosine-1-phosphate receptor-2 antagonists: therapeutic potential and potential risks. *Front Pharmacol*. 2016;7:167.
45. **Sala D**, **Cunningham TJ**, **Stec MJ**, **et al**. The Stat3-Fam3a axis promotes muscle stem cell myogenic lineage progression by inducing mitochondrial respiration. *Nat Commun*. 2019;10(1):1796.
46. **Ma JF**, **Sanchez BJ**, **Hall DT**, **Tremblay A-M**, **Di Marco S**, **Gallouzi I-E**. STAT3 promotes IFNγ/TNFα-induced muscle wasting in an NF-κB-dependent and IL-6-independent manner. *EMBO Mol Med*. 2017;9(5):622–637.
47. **Zhang L**, **Pan J**, **Dong Y**, **et al**. Stat3 activation links a C/EBPδ to myostatin pathway to stimulate loss of muscle mass. *Cell Metab*. 2013;18(3):368–379.
48. **Madaro L**, **Passafaro M**, **Sala D**, **et al**. Denervation-activated STAT3-IL-6 signalling in fibro-adipogenic progenitors promotes myofibres atrophy and fibrosis. *Nat Cell Biol*. 2018;20(8):917–927.
49. **Chalhoub D**, **Boudreau R**, **Greenspan S**, **et al**. Associations between lean mass, muscle strength and power, and skeletal size, density and strength in older men. *J Bone Miner Res*. 2018;33(9):1612–1621.
50. **Kirk B**, **Harrison SL**, **Zanker J**, **et al**. Interactions between HR-pQCT bone density and D_3 Cr muscle mass (or HR-pQCT bone structure and HR-pQCT muscle density) in predicting fractures: the Osteoporotic Fractures in Men Study. *J Bone Miner Res*. 2023;38(9):1245–1257.
51. **Hansen M**, **Rubinsztein DC**, **Walker DW**. Autophagy as a promoter of longevity: insights from model organisms. *Nat Rev Mol Cell Biol*. 2018;19(9):579–593.
52. **Plotkin LI**, **Bellido T**. Osteocytic signalling pathways as therapeutic targets for bone fragility. *Nat Rev Endocrinol*. 2016;12(10):593–605.
53. **Pérez-Baos S**, **Prieto-Potin I**, **Román-Blas JA**, **Sánchez-Pernaute O**, **Largo R**, **Herrero-Beaumont G**. Mediators and patterns of muscle loss in chronic systemic inflammation. *Front Physiol*. 2018;9:409.
54. **Kumar P**, **Kumawat RK**, **Uttam V**, **et al**. The imminent role of microRNAs in salivary adenoid cystic carcinoma. *Transl Oncol*. 2023;27:101573.
55. **Mukonzo J**, **Aklillu E**, **Marconi V**, **Schinazi RF**. Potential drug-drug interactions between antiretroviral therapy and treatment regimens for multi-drug resistant tuberculosis: Implications for HIV care of MDR-TB co-infected individuals. *Int J Infect Dis*. 2019;83:98–101.

Author information

D. Liu, MMed, Doctor
K. Wang, MMed, Doctor
J. Wang, MD, Doctor
F. Cao, MD, Doctor
L. Tao, MD, Professor
Department of Orthopedics, First Hospital of China Medical University, Shenyang, China.

Author contributions

D. Liu: Data curation, Formal analysis, Methodology, Software, Writing – original draft.
K. Wang: Investigation, Writing – original draft.
J. Wang: Data curation, Methodology.
F. Cao: Data curation, Investigation, Software.
L. Tao: Funding acquisition, Project administration, Resources, Writing – review & editing.

D. Liu and K. Wang contributed equally to this work.

Funding statement

The authors disclose receipt of the following financial or material support for the research, authorship, and/or publication of this article: support from the Liaoning Province Natural Fund (2022-YGJC-58) and Shenyang City Natural Fund (22-321-32-08).

ICMJE COI statement

All authors report support from the Liaoning Province Natural Fund (2022-YGJC-58) and Shenyang City Natural Fund (22-321-32-08), related to this study.

The authors declare that they have no known competing financial interests or personal relationships, which may affect the work reported in this article.

Data sharing

The data for this study are publicly available at: https://www.ncbi.nlm.nih.gov/gds/.

Acknowledgements

We thank the authors of the GSE1428, GSE136344, GSE172410, GSE7158, GSE56814, and GSE147287 datasets for their contribution.

Open access funding

The authors report that they received open access funding for their manuscript from the Liaoning Province Natural Fund (grant number 2022-YGJC-58) and the Shenyang City Natural Fund (grant number 22-321-32-08).